to substantiate the above interesting findings.

## V. Conclusions

A first theoretical analysis of CCNN, the fourth and last possible isomer with empirical formula $C_2N_2$, was presented in this work. At Hartree–Fock and various configuration interaction levels of theory a closed-shell ground state $^1\Sigma^+$ and a linear equilibrium geometry were confirmed. Chemical bonding was found to occur between the closed-shell monomers $C_2(^1\Sigma_g^+)$ and $N_2(^1\Sigma_g^+)$. $CCNN(^1\Sigma^+)$ must thus be classified as a normal molecule in a chemical sense, and the possible model of a van der Waals complex can be excluded unequivocally. At Hartree–Fock level, the analysis of the charge density distribution revealed a new type of binding mechanism, referred to as localizing hybridization. At all levels of calculations presented in this work, the existence of an energy barrier to unimolecular dissociation into the closed-shell monomers $C_2(^1\Sigma_g^+)$ and $N_2(^1\Sigma_g^+)$ was confirmed. The appearance of the energy barrier reflects the loss in the total energy of $CCNN(^1\Sigma^+)$ due to localizing hybridization of the $C_2(^1\Sigma_g^+)$ monomer. While the kinetical stabilization of $CCNN(^1\Sigma^+)$ is assured, we are not yet able to give a definitive statement about whether the system is also absolutely stable to unimolecular dissociation into the closed-shell monomers $C_2(^1\Sigma_g^+)$ and $N_2(^1\Sigma_g^+)$. For the most part, this uncertainty depends on the only partial incorporation of the strong electron correlation effects present at the $C_2(^1\Sigma_g^+)$ monomer. We stress that large-scale configuration interaction computations or methods of equivalent accuracy with larger basis sets should be very helpful to clarify the interesting question about whether $CCNN(^1\Sigma^+)$ is absolutely or kinetically stable to unimolecular dissociation.

We assume the $CCNN(^1\Sigma^+)$ system to be fairly reactive and to exhibit unusual chemical and physical properties. The large dipole moment, which is strongly varying with the central CN bond length of CCNN (distance between the monomers $C_2$ and $N_2$), is of particular interest. The (absolutely or kinetically) stable chemical bonding of the closed-shell molecules $C_2(^1\Sigma_g^+)$ and $N_2(^1\Sigma_g^+)$ should be of potential interest for further theoretical and experimental investigations. As an outlook, we focus the readers' attention on the $CCCO(^1\Sigma^+)$ molecule, the monomers of which are isoelectronic to those of CCNN. Investigations are in progress that indicate that the stability of the codimer $CCCO(^1\Sigma^+)$ to unimolecular dissociation depends on a binding mechanism essentially identical with the localizing hybridization scheme introduced in this work. A further interesting question may be whether the astrophysical importance of CCCO is also valid for the CCNN system.

# Photochemical Ligand Loss as a Basis for Imaging and Microstructure Formation in a Thin Polymeric Film

**Sharon Gould, Terrence R. O'Toole, and Thomas J. Meyer***

*Contribution from the Kenan Laboratories of Chemistry, University of North Carolina, Chapel Hill, North Carolina 27599-3290.* *Received May 21, 1990*

**Abstract:** Ligand loss photochemistry occurs in thin polymeric films of poly$[Ru(bpy)_2(vpy)_2]^{2+}$ (bpy is 2,2′-bipyridine, vpy is 4-vinylpyridine), poly$[Ru(Me_2bpy)_2(vpy)_2]^{2+}$ ($Me_2bpy$ is 4,4′-dimethyl-2,2′-bipyridine), and poly$[Ru(Me_4bpy)_2(vpy)_2]^{2+}$ ($Me_4bpy$ is 4,4′,5,5′-tetramethyl-2,2′-bipyridine). These films were formed by reductive electropolymerization of the corresponding 4-vinylpyridine complexes on Pt disk electrodes. Upon photolysis, the ruthenium–pyridyl bonds were cleaved and the polymer was lost, exposing the underlying substrate. The photochemical reaction was used to transfer an image to the films by using masking techniques. In a subsequent step, poly$[Os(vbpy)_3]^{2+}$ (vbpy is 4-methyl-4′-vinyl-2,2′-bipyridine), which is photochemically stable, was formed selectively in the exposed regions of the electrode by reductive electropolymerization. This procedure gave a laterally resolved, two-component, film-based structure in which there were discrete, spatially segregated regions of $Ru^{II}$ and $Os^{II}$. In a final step, the remaining film containing $Ru^{II}$ was removed by photolysis. This procedure left an image of the original mask in the poly$[Os(vbpy)_3]^{2+}$ that remained.

## Introduction

Thin films of polymeric, polypyridyl complexes of $Ru^{II}$, $Os^{II}$, or $Re^{I}$ can be prepared by well-established synthetic procedures that are based on electropolymerization on conductive substrates.[1] It has been shown that in these films the individual metal complex sites retain, to a high degree, the oxidation–reduction, light absorbance, and even reactivity characteristics of related complexes in solution. The synthetic chemistry based on electropolymerization is well developed, with procedures available for preparing multicomponent films or multilayer structures in which different components are separated in distinct layers. Even given the rapid evolution of this chemistry, an outstanding problem that remains to be solved is how to build spatially controlled, vertical structures that are perpendicular to the underlying substrate.

The photochemistry of the polypyridyl complexes in solution is well-defined and extensive.[2] It includes examples of photochemical energy conversion based on electron transfer and studies of intramolecular electron or energy transfer in complex molecular assemblies.

The photochemical reactivity also exists for individual metal-complex sites in thin polymeric films. Examples are known

(1) (a) Calvert, J. M.; Schmehl, R. H.; Sullivan B. P.; Facci, J. S.; Meyer, T. J.; Murray, R. W. *Inorg. Chem.* **1983**, *22*, 2151. (b) Denisevich, P.; Abruña, H. D.; Leidner, C. R.; Meyer, T. J.; Murray, R. W. *Inorg. Chem.* **1982**, *21*, 2153–2161. (c) Murray, R. W. *Annu. Rev. Mater. Sci.* **1984**, *14*, 145–169. (d) O'Toole, T. R.; Margerum, L. D.; Bruce, M. R.; Sullivan, B. P.; Murray, R. W.; Meyer, T. J. *J. ELectroanal. Chem. Interfacial Electrochem.* **1989**, *259*, 217–238. (e) Deronzier, A.; Moutet, J.-C. *Acc. Chem. Res.* **1989**, *22*, 249–255.

(2) (a) Juris, A.; Balzani, V.; Barigelletti, F.; Campagna, S.; Belser, P.; Von Zelewsky, A. *Coord. Chem. Rev.* **1988**, *84*, 85. (b) Kalyanasundaram, K. *Coord. Chem. Rev.* **1982**, *46*, 159. (c) Whitten, D. G. *Acc. Chem. Res.* **1980**, *13*, 83. (d) Sutin, N.; Creutz, C. *Pure Appl. Chem.* **1980**, *52*, 2717. (e) Watts, R. J. *J. Chem. Educ.* **1983**, *60*, 834. (f) Meyer, T. J. *Pure Appl. Chem.* **1986**, *58*, 1193. (g) Ferguson, J.; Herren, F.; Krausz, E.; Vrbancich, J. *Coord. Chem. Rev.* **1985**, *64*, 21. (h) Meyer, T. J. In *Progress in Inorganic Chemistry*; Lippard, S. J., Ed.; Wiley & Sons: New York, 1983, Vol. 30, p 389. (i) Meyer, T. J. *Acc. Chem. Res.* **1989**, *22*, 163.

0002-7863/90/1512-9490$02.50/0 

of excited-state electron transfer[3] and the photochemical oxidation of a metal to metal bond.[4] When compared to reactions in solution, these reactions have the distinctive property, and potential advantage, of occuring in a translationally rigid environment. The individual molecular sites are bound in the polymer matrix and occupy fixed sites that are not diffusionally labile. This introduces an element of structure to the photochemical array.

The existence of an underlying structure and the ability to change it have provided a basis for the design of photoelectrodes based on photochemical electron transfer.[3] The fixed character of the photochemically active sites has provided the basis for photochemical image formation and a photochemical/electrochemical write/erase cycle.[4]

An additional photochemical reaction that is known for polypyridyl complexes of $Ru^{II}$ is photochemical ligand loss, eq 1.[5,6]

$$[Ru(bpy)_3]^{2+} + 2Cl^- \xrightarrow{h\nu} Ru(bpy)_2Cl_2 + bpy \qquad (1)$$

The mechanism of these reactions has been investigated by temperature-dependent quantum yield and lifetime studies.[5] On the basis of these studies, it has been concluded that initial $Ru^{II} \rightarrow$ bpy metal to ligand charge-transfer (MLCT) excitation is followed by conversion to a low-lying dd state or states. The dd states provide an additional pathway for decay and are the origin of the ligand-loss photochemistry. This photochemistry is relatively unimportant for corresponding complexes of $Os^{II}$ because $10D_q$ is ~30% higher[7] and dd states are normally thermally inaccessible at room temperature.

We report here that photochemical ligand loss also occurs in polymeric films. Although the reactions are less efficient than equivalent reactions in solution, loss of pyridine from the metal ion does occur in films of poly$[Ru(bpy)_2(vpy)_2]^{2+}$, poly$[Ru(Me_2bpy)_2(vpy)_2]^{2+}$, or poly$[Ru(Me_4bpy)_2(vpy)_2]^{2+}$ (bpy is 2,2′-bipyridine, $Me_2bpy$ is 4,4′-dimethyl-2,2′-bipyridine, $Me_4bpy$ is 4,4′,5,5′-tetramethyl-2,2′-bipyridine, vpy is 4-vinylpyridine).

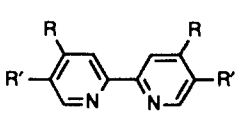

bpy: R = H, R′ = H
$Me_2bpy$: R = $CH_3$, R′ = H
$Me_4bpy$: R = $CH_3$, R′ = $CH_3$

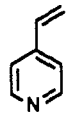

vpy

More importantly, these reactions lead to loss of the metal complex from the films and to a disruption of the polymeric network. The disruption solubilizes the polymer, and it is lost from the electrode surface. At sufficiently long photolysis times, the polymer is completely lost, exposing the underlying substrate. By using masking techniques, it is possible to create an image in the film based on the contrast between the film and the exposed electrode.

The ligand-loss-based, photochemical etching reaction provides a means for building spatially resolved structures that are perpendicular to the electrode surface. When this reaction is combined with the electropolymerization procedure in separate, sequential steps, it is possible to construct a series of dimensionally resolved, film-based structures.

## Experimental Section

**Materials.** Acetonitrile (Burdick and Jackson, UV-grade, distilled in glass) was used as received and stored in a drybox. Tetra-*n*-butylammonium hexafluorophosphate ($N(n\text{-}Bu)_4PF_6$) was precipitated from water by adding hexafluorophosphoric acid (Aldrich) to an aqueous solution of tetra-*n*-butylammonium bromide (Aldrich). The resulting precipitate was recrystallized twice from ethanol, dissolved in a minimum amount of $CH_2Cl_2$, and precipitated by addition to diethyl ether. The white solid was dried under vacuum for 72 h. Sodium dimethyldithiocarbamate was recrystallized from ethanol/diethyl ether. The compound 4,4′-dimethyl-2,2′-bipyridine ($Me_2bpy$) (Aldrich) was recrystallized from ethyl acetate and dried under vacuum. The compound 4-vinylpyridine (Aldrich) was purified before use by passage down a column of activated alumina. Synthetic procedures for the preparation of 4-methyl-4′-vinyl-2,2′-bipyridine (vbpy),[8a] $Ru(bpy)_2(Cl)_2{\cdot}2H_2O$,[8b] $[Ru(bpy)_2(vpy)_2](PF_6)_2$,[1a] and $Ru(DMSO)_4(Cl)_2$,[8c] were as described elsewhere. The compound 4,4′,5,5′-tetramethyl-2,2′-bipyridine ($Me_4bpy$) was generously provided by Walter Dressick.

**$Ru(Me_2bpy)_2(Cl)_2{\cdot}2H_2O$.** An amount of 85.4 mg (0.176 mmol) of $Ru(DMSO)_4(Cl)_2$, 65 mg (0.35 mmol) of $Me_2bpy$, and 78 mg (1.8 mmol) of LiCl was heated at reflux in 6 mL of 1-methyl-2-pyrrolidinone under argon. After 1 h the solution was cooled, and 30 mL of water was added. The solution was extracted with three 200-mL portions of $CH_2Cl_2$. The combined $CH_2Cl_2$ extracts were dried over $MgSO_4$ and filtered, after which the solution volume was reduced by rotary evaporation. The resulting residue was redissolved in a minimum amount of $CH_2Cl_2$, and the product was precipitated by addition to diethyl ether. The dark solid was filtered and dried under vacuum; dried 74%. Anal. Calcd for $Ru(Me_2bpy)_2(Cl)_2{\cdot}2H_2O$: C, 50.01; H, 4.92; N, 9.71; Cl, 13.00. Found: C, 51.02; H, 4.65; N, 9.75; Cl, 12.92.

**$Ru(Me_4bpy)_2(Cl)_2{\cdot}2H_2O$.** An amount of 208.5 mg (0.80 mmol) of $RuCl_3{\cdot}3H_2O$, 336.7 mg (1.59 mmol) of $Me_4bpy$, 500 mg (11.8 mmol) of LiCl, and 224.5 mg (2.04 mmol) of hydroquinone was dissolved in 23 mL of dimethoxyethane and 12 mL of methanol. The solution was degassed with $N_2$ for 20 min and then heated at reflux under $N_2$ for 24 h. After the solution was cooled to room temperature, ~50 mL of $H_2O$ was added. A brownish purple solid was collected by filtration and washed thoroughly with $H_2O$. The product was dissolved in ~150 mL of methylene chloride, and the solution was washed with 3 × 100 mL portions of water until the water layer remained colorless. After being dried over anhydrous $MgSO_4$, the methylene chloride layer was reduced to dryness by rotary evaporation. The dark purple product was reprecipitated from a minimum amount of methylene chloride by addition to diethyl ether, collected by filtration, and dried under vacuum; yield 56%. Anal. Calcd for $Ru(Me_4bpy)_2(Cl)_2{\cdot}2H_2O$: C, 53.16; H, 5.74; N, 8.85; Cl, 11.21. Found: C, 54.30; H, 5.94; N, 8.01; Cl, 10.78. $^1H$ NMR (200 MHz, $CD_2Cl_2$): $\delta$ 9.76 (s, 2 H), 7.90 (s, 2 H), 7.76 (s, 2 H), 7.26 (s, 2 H), 2.53 (s, 6 H), 2.46 (s, 6 H), 2.31 (s, 6 H), 1.94 (s, 6 H).

**$[Ru(Me_2bpy)_2(vpy)_2](PF_6)_2$.** To a solution of 74.8 mg (0.1 mmol) of $Ru(Me_2bpy)_2Cl_2{\cdot}2H_2O$ in 10 mL of $H_2O$ and 15 mL of ethanol was added 0.5 mL (4.7 mmol) of 4-vinylpyridine. The solution was heated at reflux for 4 h under argon. After cooling, the ethanol was removed by rotary evaporation, and an aqueous solution of $NH_4PF_6$ was added. The resulting orange precipitate was collected by filtration and purified by column chromatography on an alumina column with 2:1 toluene/acetonitrile as eluent. After evaporation, the product was redissolved in a minimum amount of acetonitrile and reprecipitated by dropwise addition to stirring diethyl ether. The orange solid was collected by filtration and dried under vacuum. Anal. Calcd for $[Ru(Me_2bpy)_2(vpy)_2](PF_6)_2$: C, 47.06; H, 3.95; , 8.67. Found: C, 46.56; H, 4.07; N, 8.56. $^1H$ NMR (200 MHz, $CD_2Cl_2$): $\delta$ 8.70 (d, 2 H, 6 Hz), 8.15 (d, 4 H, 7 Hz), 8.07 (s, 2 H), 7.99 (s, 2 H), 7.72 (d, 2 H, 6 Hz), 7.64 (d, 2 H, 6 Hz), 7.30 (d, 4 H, 7 Hz), 7.23 (d, 2 H, 6 Hz), 6.65 (dd, 2 H, 10 and 18 Hz), 6.04 (d, 2 H, 18 Hz), 5.61 (d, 2 H, 10 Hz), 2.66 (s, 6 H), 2.50 (s, 6 H).

**$[Ru(Me_4bpy)_2(vpy)_2](PF_6)_2$.** To a solution of 124.9 mg (0.2 mmol) of $Ru(Me_4bpy)_2Cl_2{\cdot}2H_2O$ and 22.9 mg (0.21 mmol) of hydroquinone in 5 mL of $H_2O$ and 10 mL of ethanol was added 1.0 mL (9.4 mmol) of 4-vinylpyridine. The solution was heated at reflux for 6 h under argon. After cooling, the ethanol was removed by rotary evaporation, and an aqueous solution of $NH_4PF_6$ was added. The resulting orange precipitate

(3) (a) Margerum, L. D.; Meyer, T. J.; Murray, R. W. *J. Electroanal. Chem. Interfacial Electrochem.* **1983**, *149*, 279–285. (b) Oyama, N.; Yamaguchi, S.; Kaneko, M.; Yamada, A. *J. Electroanal. Chem. Interfacial Electrochem.* **1982**, *139*, 215. (c) Majda, M.; Faulkner, L. R. *J. Electroanal. Chem. Interfacial Electrochem.* **1982**, *137*, 149. (d) Surridge, N. A.; Hupp, J. T.; McClanahan, S. F.; Gould, S.; Meyer, T. J. *J. Phys. Chem.* **1989**, *93*, 304–313.

(4) O'Toole, T. R.; Sullivan, B. P.; Meyer, T. J. *J. Am. Chem. Soc.* **1989**, *111*, 5699–5706.

(5) (a) Van Houten, J.; Watts, W. J. *Inorg. Chem.* **1978**, *17*, 3381. (b) Durham, B.; Casper, J. V.; Nagle, J. K.; Meyer, T. J. *J. Am. Chem. Soc.* **1982**, *104*, 4803–4810. (c) Hoggard, P. E.; Porter, G. B. *J. Am. Chem. Soc.* **1978**, *100*, 1457.

(6) (a) Bosnich, B.; Dwyer, F. P. *Aust. J. Chem.* **1966**, *19*, 2229. (b) Gleria, M.; Minto, F.; Beggiato, G.; Bortolus, P. *J. Chem. Soc., Chem. Commun.* **1978**, 285. (c) Durham, B.; Walsh, J. L.; Carter, C. L.; Meyer, T. J. *Inorg. Chem.* **1980**, *19*, 860–865. (d) Pinnick, D. V.; Durham, B. *Inorg. Chem.* **1984**, *25*, 1440–1445.

(7) (a) Ballhausen, C. J. *Introduction to Ligand Fields*; McGraw-Hill: New York, 1962. (b) Lever, A. B. P. *Inorganic Electronic Spectroscopy*, 2nd ed.; Elsevier: New York, 1984.

(8) (a) Abruña, H. D.; Breikess, A. I.; Collum, D. B. *Inorg. Chem.* **1985**, *24*, 987, 988. (b) Sullivan, B. P.; Salmon, D. J.; Meyer, T. J. *Inorg. Chem.* **1978**, *17*, 3334–3341. (c) Evans, I. P.; Spencer, A.; Wilkinson, G. *J. Chem. Soc., Dalton Trans.* **1973**, 204–209.

Table I. Half-Wave Potentials (±0.02 V) vs $Ag/AgNO_3$[9] for the Redox Couples in Thin Polymeric Films in $N(n\text{-}Bu_4)PF_6/CH_3CN$ at Room Temperature

| film | $E_{1/2}^{(1)}(M^{III/II})$, V | $E_{1/2}^{(2)}(bpy^{0/-})_1$, V | $E_{1/2}^{(3)}(bpy^{0/-})_2$, V |
|---|---|---|---|
| $poly[Ru(bpy)_2(vpy)_2]^{2+}$ | +1.01 | -1.61 | -1.79 |
| $poly[Ru(Me_2bpy)_2(vpy)_2]^{2+}$ | +0.89 | -1.71 | -1.90 |
| $poly[Ru(Me_4bpy)_2(vpy)_2]^{2+}$ | +0.80 | -1.89 | -2.05 |
| $poly[Os(vbpy)_3]^{2+}$ | +0.46 | -1.57 | -1.76 |

was collected by filtration and purified by column chromatography on an alumina column with 2:1 toluene/acetonitrile as eluent. After evaporation, the product was redissolved in a minimum amount of acetonitrile and reprecipitated by dropping into stirring diethyl ether. The product was an orange powder; yield 72%. Anal. Calcd for $[Ru(Me_4bpy)_2(vpy)_2](PF_6)_2$: C, 49.18; H, 4.52; N, 8.19. Found: C, 47.95; H, 4.50; N, 7.91. $^1H$ NMR (200 MHz, $CD_3CN$): $\delta$ 8.50 (s, 2 H), 8.23 (d, 4 H, 6.6 Hz), 8.07 (s, 2 H), 7.99 (s, 2 H), 7.46 (s, 2 H), 7.23 (d, 4 H, 6.6 Hz), 6.69 (dd, 2 H, 11.0 and 17.6 Hz), 6.08 (d, 2 H, 17.6 Hz), 5.58 (d, 2 H, 10.9 Hz), 2.48 (s, 6 H), 2.38 (s, 6 H), 2.33 (s, 6 H), 2.08 (s, 6 H).

**$[Os(vbpy)_3](PF_6)_2$.** A solution of 174 mg (0.38 mmol) of $(NH_4)(OsCl_6)$ and 240 mg (1.22 mmol) vbpy in 8 mL of ethylene glycol was degassed with Ar and heated at reflux for 3 h. The solution was cooled, and aqueous $NH_4PF_6$ was added. The resulting brown solid was collected by filtration and washed with diethyl ether. The product was purified on an alumina column by using 1:1 toluene/acetonitrile as the eluent; yield 28%. Anal. Calcd for $[Os(vbpy)_3](PF_6)_2$: C, 43.82; H, 3.40; N, 7.86. Found: C, 43.82; H, 3.57; N, 7.78.

**$[Ru(Me_4bpy)_2(dmtc)](PF_6)$.** A solution of 79.2 mg (0.125 mmol) of $Ru(Me_4bpy)_2(Cl)_2 \cdot 2H_2O$ and 79.9 mg (0.446 mmol) of sodium dimethyldithiocarbamate in 8 mL of ethanol and 6 mL of water was heated at reflux under argon for 3 h. The solution was cooled, and $NH_4PF_6$ was added. A dark red precipitate appeared and was collected by filtration, rinsed with water, and dried under vacuum overnight. The product was purified by column chromatography on an alumina column with 2:1 toluene/acetonitrile as eluent. Chromatography separated two products from the reaction mixture; a green band was eluted first from the column, followed by a brick red band. The brick red band was collected and evaporated and the product reprecipitated from acetonitrile in diethyl ether; yield 60%. Anal. Calcd for $[Ru(Me_4bpy)_2(dmtc)](PF_6)$: C, 47.08; H, 4.84; N, 8.85; F, 14.42; S, 8.11. Found: C, 46.35; H, 4.79; N, 8.59; F, 14.21; S, 7.75.

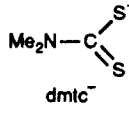


dmtc⁻

**Measurements. Preparation and Characterization of the Films.** $^1H$ NMR data were recorded in $CD_2Cl_2$ (Aldrich) or $CD_3CN$ (Cambridge Isostopes) as solvents with Bruker AC200 or Varian XL400 spectrometers. A Hewlett-Packard Model 8451A diode array spectrophotometer was used to record routine electronic spectra. When absorption spectra of the polymeric films were measured, light-scattering effects were minimized by including a clean ITO electrode in the reference scan and utilizing a cell equipped with an electrode holder for reproducible positioning of the electrode in the optical train. Cyclic voltammetric experiments were carried out by using a Princeton Applied Research Model 174A polarographic analyzer and a home-built wave-form generator. Voltammograms were recorded on a Hewlett-Packard 7015B X-Y recorder. All potentials are relative to the $Ag/AgNO_3$ reference electrode[9] unless otherwise noted. The electrodes used in the electrochemical experiments were 0.12-$cm^2$ Teflon-shrouded Pt disks. The disk electrodes were polished with 1-$\mu$m diamond paste (Buehler) and rinsed with $H_2O$ and acetone prior to use. UV–visible spectra were acquired on optically transparent electrodes of indium-doped tin oxide (ITO) (Delta Technologies, Ltd.). In surface analysis studies, ITO and Pt flag electrodes were used in addition to the Teflon-shrounded Pt disk electrodes.

Formation of the polymeric films by electropolymerization was carried out in a one-compartment cell containing acetonitrile solutions of the monomer in the range 0.2–2.0 mM. Films of $poly[Ru(bpy)_2(vpy)_2](PF_6)_2$ were deposited by cycling the potential of the working electrode between -1.0 and -2.0 V at scan rates of 50–100 mV/s. For $[Ru(Me_2bpy)_2(vpy)_2]^{2+}$ or $[Ru(Me_4bpy)_2(vpy)_2]^{2+}$, the potential limit on the reductive side was -2.1 V. All experiments were carried out under a $N_2$ atmosphere in a Vacuum Atmospheres glovebox that had been modified so as to be under a constant $N_2$ purge. The surface coverage of polymer on the electrode ($\Gamma_{Ru}$) was determined by integration of the charge under the $Ru^{III/II}$ wave in a cyclic voltammogram measured in a fresh electrolyte-containing solution.

Typical surface coverages were $3 \times 10^{-8}$ mol/$cm^2$, which corresponds to ~100–300 monolayers by assuming a value of $10^{-10}$ mol/$cm^2$ per monolayer. The number of reductive scans necessary to achieve those coverages decreased in the order $[Ru(bpy)_2(vpy)_2]^{2+} > [Ru(Me_2bpy)_2(vpy)_2]^{2+} > [Ru(Me_4bpy)_2(vpy)_2]^{2+}$, as expected on the basis of initial reduction at the bpy.[1a,b] No significant change in peak height or wave shape was observed in successive cyclic voltammetric scans through the $Ru^{III/II}$ waves in 0.1 M $N(n\text{-}Bu_4)PF_6$/acetonitrile. The films were less stable reductively, especially for films that contained the methyl-substituted bipyridine ligands. Films of $poly[Ru(bpy)_2(vpy)_2]^{2+}$ could be cycled through the bpy-based reductions several times with little to no change in the current response of the $Ru^{III/II}$ wave upon a return scan. Cycling a film of $poly[Ru(Me_4bpy)_2(vpy)_2]^{2+}$ from +1.4 to -2.2 V led to a 50% decrease in the magnitude of the $Ru^{III/II}$ wave upon a return scan. When electrochemical measurements were used for analysis, the measurements were made in potential ranges where the films were stable.

**Photoimaging.** Light-generated patterns were created by photolysis of $poly[Ru(Me_4bpy)_2(vpy)_2]^{2+}$ on ITO or Pt electrodes that were immersed in a 0.1 M aqueous solution of $dmtc^-$. The electrodes were suspended in a glass cell, which, except for its bottom, had been covered with black electrical tape. A homemade mask that consisted of an array of four holes, 0.53-mm in diameter with a center to center separation of 0.16 cm, in a thin (0.2-mm) piece of black Phenolic was inserted into the bottom of the cell. The electrode was positioned over a portion of the mask and lowered until it was near (<1 mm) but not touching the bottom of the cell. Photolyses were carried out by using a Bausch and Lomb Model SP 200 mercury lamp. The output from the lamp was passed through a Pyrex UV-cutoff filter before reaching the sample. Typically, the films were irradiated for 15–45 min depending on the starting film thicknesses. After irradiation, the image was developed by rinsing the electrode in water and acetonitrile.

Electropolymerization of $poly[Os(vbpy)_3]^{2+}$ into the photogenerated pattern was carried out in a glovebox by cycling the imaged electrode in a 0.5 mM solution of $[Os(vbpy)_3]^{2+}$ in acetonitrile between -0.9 and -1.75 V vs $Ag/AgNO_3$ at a scan rate of 100 mV/s. Typically, 15–20 cycles were used.

In order to explore spatial resolution and dimensionality, line patterns were generated on ITO and Pt flag electrodes. The mask was a chrome on glass resolution-testing target (NBS 1963A) (Rolyn Optics Co.). Irradiation times were ~2 min in 0.1 M aqueous $dmtc^-$ solutions, after which the electrodes were rinsed in $H_2O$ and $CH_3CN$. Step profilometry experiments were performed on a Tencor Alpha Step 100 profilometer. The stylus tip was 12.5 $\mu$m. Photographs of the electrode surfaces were taken through the phototube of an Olympus STZR stereomicroscope with a Nikon FG 35-mm camera.

**Photoimaging in Dry Films.** Images were also generated in films irradiated in the absence of solvent. The films were prepared by soaking in a 0.05–0.1 M acetonitrile solution of sodium dimethyldithiocarbamate for 2 h. After being rinsed in acetonitrile, the films were allowed to air dry for at least 30 min. The electrode was placed directly on the mask, irradiated, typically for 15–40 min, and developed as before.

**Surface Analysis.** Small-spot X-ray photoelectron spectroscopy (XPS) was performed with a Perkin-Elmer Physical Electronics Model 5400. The spot size was 200 $\mu$m. Scanning electron microscopy (SEM) was carried out by using an ISI DS-130. A beam energy of 9 kV was used.

## Results

**Electrochemistry.** In Table I are summarized the formal potentials obtained by cyclic voltammetry for the oxidative and reductive couples that appear for electrodes coated with thin polymeric films of $poly[Ru(Me_4bpy)_2(vpy)_2]^{2+}$, $poly[Ru(Me_2bpy)_2(vpy)_2]^{2+}$, or $poly[Ru(bpy)_2(vpy)_2]^{2+}$. The potentials for both the $Ru^{III/II}$ ($E_{1/2}^{(1)}$) and the bpy-based, reductive couples ($E_{1/2}^{(2)}$, $E_{1/2}^{(3)}$) are shifted negatively for methyl-substituted bipyridine ligands. This is an electronic substituent effect arising from the greater electron-donating ability of $-CH_3$ compared to -H. Its magnitude is ~-25 mV per methyl substituent.

(9) The $Ag/AgNO_3$ reference electrode was 0.01 M in $AgNO_3$ in 0.1 M $NEt_4PF_6$/acetonitrile. The potential of this electrode vs SSCE is +0.3 V.

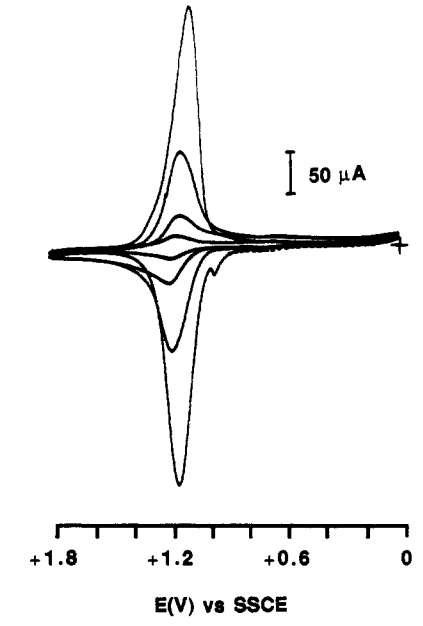


**Figure 1.** Cyclic voltammograms recorded in 0.1 M $N(n\text{-}Bu)_4PF_6/CH_3CN$ for a poly$[Ru(Me_4bpy)_2(vpy)_2]^{2+}$ film following photolysis at 436 nm: $I^o$ = 1.17 einsteins/s·cm$^2$; scan rate = 100 mV/s. Voltammograms were recorded at $t$ = 0, 10, 18, and 31 s. Each of the scans shown was recorded after an initial "conditioning" cycle.

**Photochemistry.** When a Pt-disk electrode coated with a thin film of poly$[Ru(Me_4bpy)_2(vpy)_2]^{2+}$ was immersed in a solution of 0.1 M $N(n\text{-}Bu)_4PF_6$ in acetonitrile and photolyzed at 436 nm, the peak current for the reversible $Ru^{III/II}$ wave at 1.0 V vs $Ag/AgNO_3$ in cyclic voltammograms decreased with time; see Figure 1. Loss of the film-based couple was also observed when films were photolyzed in water or in solutions that contained the potentially coordinating anions $Cl^-$, $SO_4^{2-}$, or dimethyldithiocarbamte (dmtc$^-$).

The net photochemistry involves cleavage of ruthenium–pyridyl bonds with concomitant loss of the metal complex unit from the films, eq 2. The properties of related complexes toward photo-

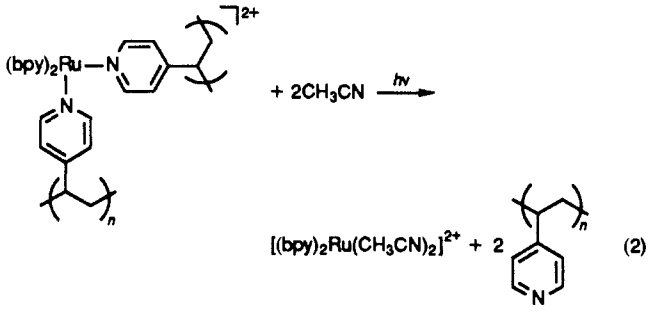


(2)

chemical ligand loss in solution have been established.[5,6] Photolysis of $[Ru(bpy)_2(py)_2]^{2+}$ (py is pyridine) in $CH_2Cl_2$ in the presence of various anions, $X^-$ (=$Cl^-$, $NCS^-$, ...), causes the stepwise photochemical substitution of $X^-$ for py to occur. In the films, photosubstitution at the metal leads to the loss of the complex. The poly(vpy) fragments that remain following loss of the complex are of sufficiently short chain length that they are soluble in the photolysis medium. That they are lost from the electrode surfce was demonstrated by XPS measurements, see the following text.

In experiments where the photolysis medium was aqueous dmtc$^-$, the appearance of the photoproduct could be followed spectrophotometrically. It is insoluble in water and is retained in the film. In Figure 2 are shown spectra of poly$[Ru(Me_4bpy)_2(vpy)_2]^{2+}$ on an indium tin oxide transparent electrode as a function of photolysis time. The appearance of $[Ru(Me_4bpy)_2(dmtc)]^+$ was shown by the increase in absorbance at 508 nm, which is a $\lambda_{max}$ for this complex. The complex, presumably as the dmtc$^-$ salt, remained on the surface when exposed to water but was readily removed by rinsing with acetonitrile.

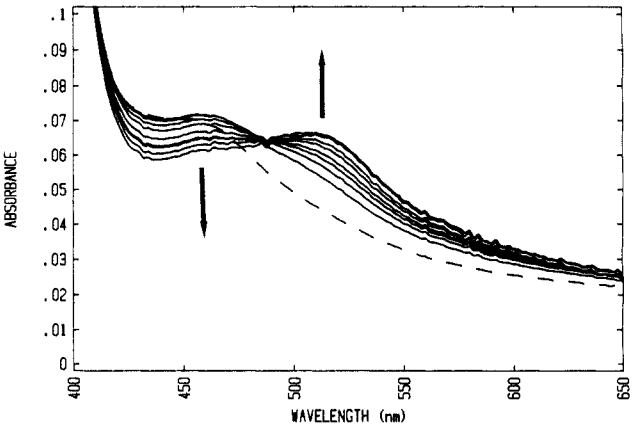


**Figure 2.** Electronic absorption spectra of a poly$[Ru(Me_4bpy)_2(vpy)_2]^{2+}$ film ($\Gamma_{Ru}$ = 6.8 × 10$^{-9}$ mol/cm$^2$) at various times over a photolysis (460-nm) period of 58 min. The external solution was 0.1 M aqueous dmtc$^-$. The dashed line (- - -) shows the initial spectrum.

The photochemical loss of poly$[Ru(bpy)_2(vpy)_2]^{2+}$ with 0.1 M $Cl^-$ in the external solution was also followed by cyclic voltammetry. After photolysis in water, cyclic voltammograms were acquired in 0.1 M $NEt_4ClO_4$/acetonitrile. In these voltammograms, a wave appeared at +0.78 V vs SSCE as the complex and film were lost from the electrode. This $E_{1/2}$ value coincides with the potential of the $Ru^{III/II}$ couple in poly$[Ru(bpy)_2(vpy)(Cl)]^+$.[1a]

The kinetics of the loss of poly$[Ru(Me_4bpy)_2(vpy)_2]^{2+}$ from the films were studied with 0.1 M dmtc$^-$ in the external aqueous solution. Analysis of the data for a number of films gave per photon absorbed quantum yields, $\Phi$, in the range 0.002–0.009. By comparison, loss of the first pyridyl ligand from $[Ru(bpy)_2(py)_2]^{2+}$ in $CH_2Cl_2$ in the presence of Y (Y = $NCS^-$, $Cl^-$, or $NO_3^-$) to give $[Ru(bpy)_2(py)(Y)]^+$ occurs with $\Phi$ = 0.18 ± 0.02.[5c] The mechanistic details associated with the ligand-loss photochemistry are currently under investigation.[10]

**Photoimaging and Microstructure Formation.** The ligand-loss photochemistry was carried out with spatial control by using masking techniques. This created a basis for preparing patterns on the underlying conductive substrate. In the procedure, poly$[Ru(Me_4bpy)_2(vpy)_2]^{2+}$ was left in the masked areas and the contrast was provided by the regions of exposed electrode in the photolyzed areas.

In one set of experiments, a homemade mask was used. It consisted of a 4 × 4 array of holes, 0.53 mm in diameter with a center to center separation of 0.16 cm, in a thin (0.2-mm) piece of black Phenolic. In parts A and B of Figure 3 are shown cyclic voltammograms of a film before and after photolysis. The loss of an appreciable amount of the complex is shown in Figure 3B by the decrease in peak current for the $Ru^{III/II}$ couple. From the relative peak currents in Figure 3 parts A and B, ~30% of the overall film coverage was lost during the photolysis procedure, in addition to that lost in the photolyzed areas. The loss in the unphotolyzed regions may come largely from light scattering off the exposed electrode.

Spatially resolved X-ray photoelectron spectroscopy (XPS) on Pt flag electrodes was used to confirm that the film had been removed from the photolyzed regions. In films of poly$[Ru(Me_4bpy)_2(vpy)_2]^{2+}$, photoelectron peaks for N 1s and Ru 3d appear at 400.7 and 281.6 eV, respectively. In the photolyzed regions of the imaged electrode, both of these peaks were absent and a Pt 4f peak for the substrate was observed at 71.0 eV.

The topography of an imaged film was examined by profilometry. The trace shown in Figure 4 was recorded for a film of poly$[Ru(Me_4bpy)_2(vpy)_2]^{2+}$ on ITO after a line pattern had been

(10) Gould, S.; Meyer, T. J. Work in progress.

(11) The profilometer trace may not have provided a faithful representation of the lateral dimensions of the polymeric line. Distortions due to the dimensions of the stylus are often observed in these measurements. A typical distortion is one where the step is observed to be wider at the bottom than at the top, giving a shape similar to the one seen in Figure 4.

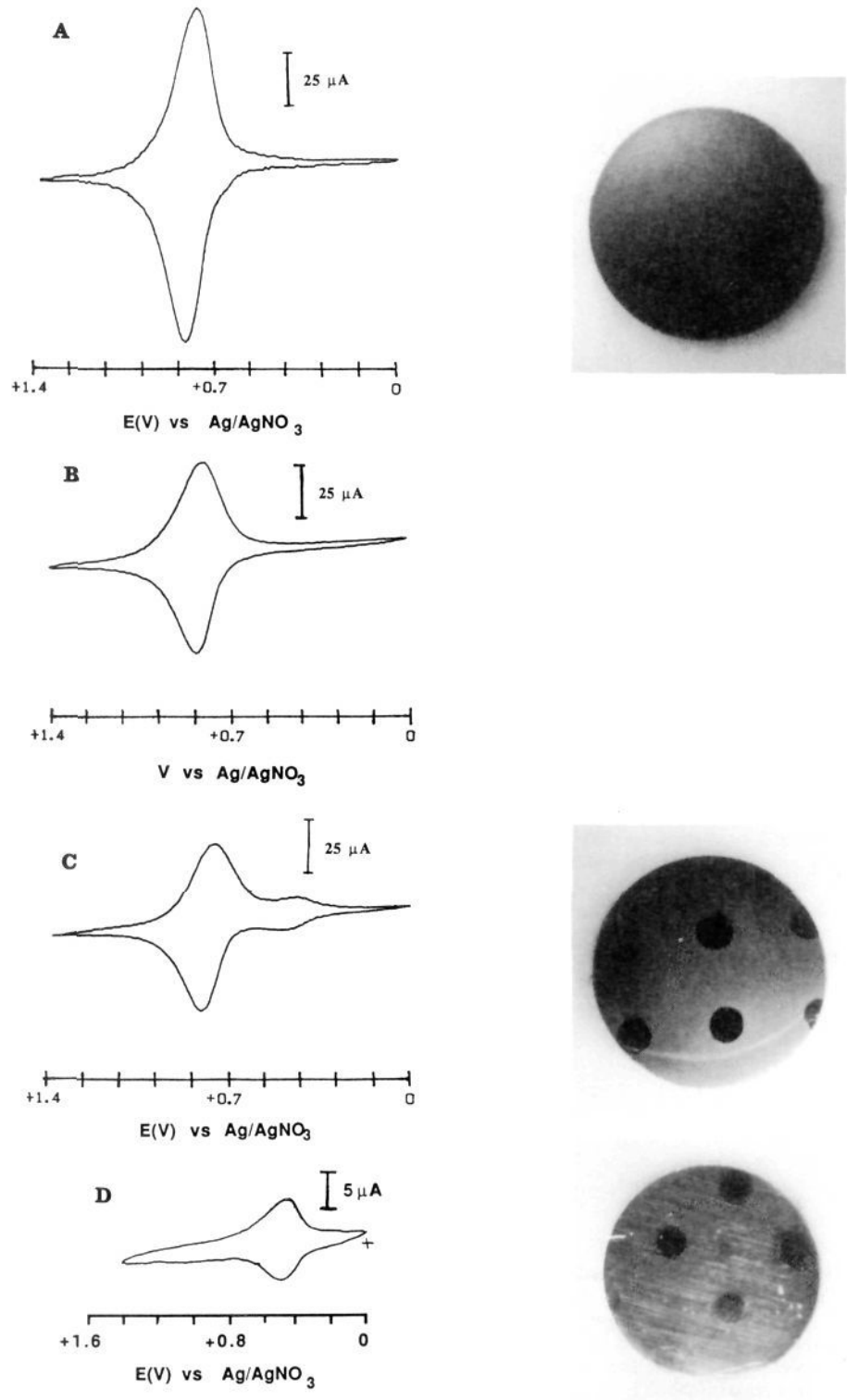


**Figure 3.** Photographs and cyclic voltammograms of Teflon-shrouded Pt disk electrodes at various stages in the photochemical/electrochemical sequence for the formation of spatially controlled microstructures. The diameter of the electrode was 0.4 cm. The mask was a 4 × 4 array of holes, 0.53 mm in diameter with a center to center separation of 0.16 cm: (A) Initial poly$[Ru(Me_4bpy)_2(vpy)_2]^{2+}$ film. (B) The film in A after photolysis in 0.1 M aqueous $dmtc^-$. The optical photograph of this film was indistinguishable from that of C. (C) The film in B after poly$[Os(vbpy)_3]^{2+}$ had been electropolymerized into the "holes" created at stage B. (D) Remaining poly$[Os(vbpy)_3]^{2+}$ on the bare Pt electrode after photolysis without a mask. The striations observed in this photograph are scratches in the Pt surface. Cyclic voltammograms were recorded in 0.1 M $N(n\text{-}Bu)_4PF_6/CH_3CN$. Scan rate = 50 mV/s.

generated photochemically by using a commercial resolution-testing target as the mask. Changes in film thickness on the order of 500 Å were observed in stepping between the photolyzed and unphotolyzed regions of the film.

After the underlying electrode had been developed photochemically, it was possible to grow a second polymer in the exposed areas by utilizing a second electropolymerization step. When an imaged electrode in a solution containing $[Os(vbpy)_3]^{2+}$ was cycled in 0.1 M $N(n\text{-}Bu)_4PF_6/CH_3CN$ from 0 to −1.75 V vs $Ag/AgNO_3$ at 100 mV/s, poly$[Os(vbpy)_3]^{2+}$ appeared in the exposed areas,

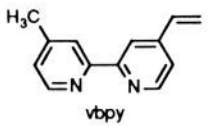

vbpy

Figure 3C. The first bpy-based reductions of $[Os(vbpy)_3]^{2+}$ and $[Ru(Me_4bpy)_2(vpy)_2]^{2+}$ occur at −1.57 and −1.80 V, respectively. The shift to a more negative potential allowed for the osmium complex to be electropolymerized selectively at the electrode surface and not on top of the remaining ruthenium polymer. At the completion of the photochemical/electrochemical cycle, waves appear for both the $Ru^{III/II}$ and $Os^{III/II}$ couples in cyclic voltammograms. As shown in Figure 3C, the $Os^{III/II}$ couple appears at +0.46 V.

By using a second photochemical cycle and photolyzing the entire electrode, it was possible to remove the remaining poly-$[Ru(Me_4bpy)_2(vpy)_2]^{2+}$ from the electrode surface. Since poly-$[Os(vpy)_3]^{2+}$ is photochemically stable, it remained on the electrode in the pattern of the original mask. The loss of poly$[Ru(Me_4bpy)_2(vpy)_2]^{2+}$, retention of poly$[Os(vbpy)_3]^{2+}$, and exposure of the bare electrode were confirmed by spatially resolved XPS. Photoelectron peaks for Os 4f at 51.5 eV and N 1s at 401.0 eV were observed in regions of the electrode where poly$[Os(vbpy)_3]^{2+}$ had been deposited into the photochemically generated image. In areas where the Pt electrode had been exposed, no Os, Ru, or N was detected; however, a peak at 71.3 eV for Pt 4f was observed. The energies for the N 1s and Pt 4f peaks were identical with the XPS results reported above within experimental error and agree well with reported literature values. A photograph and cyclic voltammogram are shown in Figure 3D.

The dimensions of the photoimage produced by the homemade mask were in good agreement with the dimension of the mask. The average diameters of the "holes" in Figure 3B and the poly$[Os(vbpy)_3]^{2+}$ "spots" in Figure 3D are ~0.56 and ~0.54 mm, compared to the diameter of the holes in the mask of 0.53 mm. The commercial line-pattern target gave a similar agreement. The profilometry trace shown in Figure 4 was used to measure the dimensions of the polymeric "lines" remaining on the electrode surface.[12] On the basis of the dimensions of the trace at the top of the step, the polymeric line was ~500 Å thick and approximately 200 μm wide. The widths of the lines of the target were 280 μm. In a related experiment on a Pt flag electrode, the widths of the polymeric lines were found to be ~0.42 mm by scanning electron microscopy compared to the 0.46-mm-wide lines of the mask.

**Photoimaging in Dry Films.** The photochemical ligand substitution reaction also occurred in films that were irradiated in the absence of solvent. In this experiment, an electrode coated with a thin film of poly$[Ru(Me_4bpy)_2(vpy)_2]^{2+}$ was soaked in an acetonitrile solution that contained $dmtc^-$. After 2 h, the electrode was removed, rinsed with $CH_3CN$, and allowed to dry. It was then irradiated with a 200-W Hg lamp equipped with a Pyrex UV cutoff filter. Visual inspection of the electrode after it had been rinsed in $H_2O$ and $CH_3CN$ showed that the pattern of the mask had been transferred to the electrode surface. In Figure 5 is shown a photograph of an imaged electrode prepared in this manner.

The successful removal of the polymeric film from irradiated regions of the electrode was dependent upon the anion used in the experiment. In an experiment where $Cl^-$ was used in place of $dmtc^-$, irradiation of the dry film resulted in only partial loss of the film. While the pattern of the image could be seen, a film coating in the irradiated regions was easily discerned, indicating that loss of the polymer from the photolyzed regions was not complete. A cyclic voltammogram of the irradiated film showed a wave at +0.32 V, which corresponds to the $Ru^{III/II}$ couple of poly$[Ru(Me_4bpy)_2(vpy)(Cl)]^+$, in addition to the $Ru^{III/II}$ couple of poly$[Ru(Me_4bpy)_2(vpy)_2]^{2+}$, which appears at +0.8 V.

(12) (a) Haas, O.; Vos, J. G. *J. Electroanal. Chem. Interfacial Electrochem.* **1980**, *113*, 139–149. (b) Haas, O.; Zumbrunnen, H. R.; Vos, J. G. *Electrochim. Acta* **1985**, *30*, 1551–1554. (c) Haas, O.; Kriens, M.; Vos, J. G. *J. Am. Chem. Soc.* **1981**, *103*, 1318, 1319.

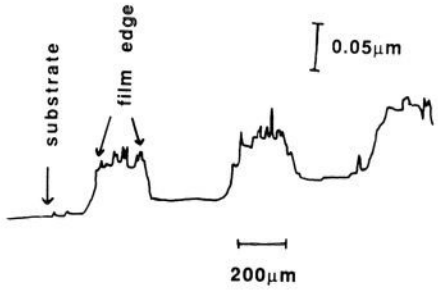


**Figure 4.** Step profilometry of a film of poly$[Ru(Me_4bpy)_2(vpy)_2]^{2+}$ on an ITO electrode after photolysis as in Figure 3B but with the use of a commercial resolution testing target as the mask. The line pattern of the mask used to generate the image was 1.8 cycles/mm, which corresponds to a line width of ~278 μm. The width of the polymeric "line" of the image at the top of the step is ~200 μm.[11]

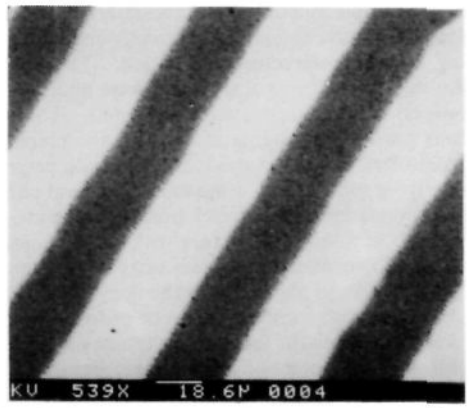


**Figure 5.** SEM of an imaged poly$[Ru(Me_4bpy)_2(vpy)_2]^{2+}$ film on a Teflon-shrouded Pt disk electrode. The photochemical imaging was accomplished by photolysis of the *dry* film, which had previously been soaked in an acetonitrile solution of $dmtc^-$, rinsed, and air dried. The line pattern of the mask was 18 cycles/mm (line width = 26 μm). The widths of the polymeric "lines" in the photograph are 27 ± 1 μm. The undulations observed at the edges of the pattern are present in the mask.

## Discussion

**Photochemical Ligand Loss in Thin Films.** Photochemical ligand loss in solution is a well-documented reaction for polypyridyl complexes of $Ru^{II}$.[5,6] The mechanism involves initial metal to ligand ($Ru^{II} \rightarrow$ bpy) charge-transfer (MLCT) excitation followed by conversion to near-lying dd states. It is the dd states that are responsible for the ligand-loss photochemistry. For *cis*-$[Ru(bpy)_2(py)_2]^{2+}$, it has been shown that the photochemical loss of the pyridyl groups occurs stepwise by the sequential displacement of py by $Y^-$ (=$Cl^-$, $NCS^-$, ...).

$$Ru(bpy)_2(py)_2^{2+} + Y^- \xrightarrow{h\nu} Ru(bpy)_2(py)(Y)^+ + py$$

$$Ru(bpy)_2(py)(Y)^+ + Y^- \rightarrow Ru(bpy)_2(Y)_2 + py$$

The ligand-loss photochemistry also occurs in films of poly-$[Ru(bpy)_2(vpy)_2]^{2+}$ and related derivatives, apparently by a closely related mechanism. The intervention of ligand-loss photochemistry was established by the spectrophotometric experiment where $[Ru(Me_4bpy)_2(dmtc)]^+$ appeared as a photoproduct upon photolysis of poly$[Ru(Me_4bpy)_2(vpy)_2]^{2+}$ with aqueous $dmtc^-$ in the external solution. The stepwise nature of the ligand loss was demonstrated by the experiments where $Cl^-$ was used as the entering group and poly$[Ru(bpy)_2(vpy)(Cl)]^+$ appeared as an intermediate.

The observation that ligand-loss photochemistry leads to loss of the ruthenium complex from the polymeric film is in contrast to an earlier report by Vos and Haas concerning photosubstitution in polymeric films of $[Ru(bpy)_2(PVP)_2]^{2+}$ (PVP is poly(4-vinylpyridine)) on electrodes.[12] In their experiments, photo-

**Scheme I**

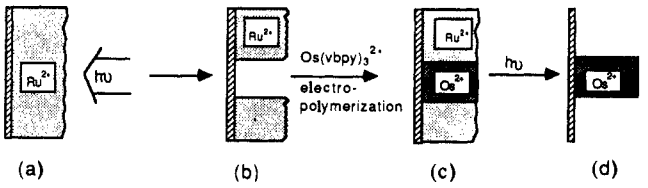


chemical displacement of one pyridine by solvent (S) resulted in essentially quantitative conversion of $[Ru(bpy)_2(PVP)_2]^{2+}$ into $[Ru(bpy)_2(PVP)(S)]^{2+}$, which was retained in the films. However, their polymeric backbone was of high molecular weight. The difference between their result and ours can be understood by assuming that the electropolymerization process gives short polymeric chains that are cross-linked by coordination to the metal center. Photolysis disrupts the cross-linking by cleaving the ruthenium–pyridyl bonds. The resulting low molecular weight oligomers are soluble and dissolve in the external solution. The chemical nature of these oligomers is currently under investigation.

**Imaging and Microstructure Formation.** The sequence of photochemical/electrochemical steps that were undertaken in the imaging experiments is illustrated in Scheme I. This sequence of reactions provides a systematic basis for the preparation of spatially controlled microstructures in the dimension perpendicular to the underlying substrate by using molecular level photochemistry. The combination of reactions—transfer of the image of the mask, synthesis of a second structure with spatial control, photochemical development of a secondary image—is reminiscent of some of the key steps in photoresist technology. In this case, the sequence of steps allows for the preparation of spatially controlled microstructures in which the separate molecular constituents have well-established and potentially exploitable light absorptivity, emission, electron transfer or even catalytic properties.

From the results of the XPS experiments, complete loss of the polymeric film occurs in the photolyzed regions of the film in the photochemical step a → b in Scheme I. It is this step that provides a basis for the transferral of the image to the electrode. At the spatial resolution of the 0.02–0.5-mm patterns that were investigated, there was a faithful replication of the negative of the mask image in the film.

Although the image-forming reaction is based on molecular level photochemistry, the ultimate resolution available in this approach remains to be established. For example, there is no guarantee that the photochemistry can be constrained to a single site following excitation at the molecular level. There is the possibility that rapid transfer of the initial excitation may occur to adjacent sites by energy-transfer hopping.

In the second stage, b → c, $[Os(vbpy)_3]^{2+}$ was electropolymerized onto the bare regions of the electrode that were exposed in the first stage. This procedure resulted in the formation of a laterally resolved structure in which there were spatially segregated domains of $Ru^{II}$ and $Os^{II}$. There are inherent limitations in forming this secondary structure. The choice of components and the potential used for the electropolymerization are critical. The material to be deposited in the photogenerated pattern must not be capable of facile diffusion through the ruthenium layer that remains on the electrode. In addition, the potential required for the second electropolymerization must lie in a region where the remaining ruthenium polymer is not itself electroactive. This condition is necessary if deposition of the polymer on the $Ru^{II}$ layer, as well as at the exposed electrode, is to be avoided.

The third, and final, stage of the sequence, c → d, involves a second photolysis but over the whole electrode surface as a way of removing the initially masked poly$[Ru(Me_4bpy)_2(vpy)_2]^{2+}$. This reaction is selective at $Ru^{II}$ because of the photostability of the $Os^{II}$ complex. The result of the second photochemical step is to create the original image of the mask, but now as poly$[Os(vbpy)_3]^{2+}$ on the electrode surface.

**Acknowledgment** is made to the Army Research Office under Grant No. DAAL03-88-K-0192 for support of this work and to Susan Maybury for providing the XPS results, Vicki Guarisco for providing the SEM results, and Dan Dohmeier for help with the photography. XPS instrumentation was funded by an instrumentation grant (R. W. Linton, Principal Investigator) from the office of Naval Research, ONR No. N00014-86-G-0200 (Grant No. 35739).